Synthesis, radiochemical and biological characteristics of ^{99m}Tc-8-hydroxy-7-substituted quinoline complex: a novel agent for infection imaging

M. A. Motaleb · E. S. Alabdullah · W. A. Zaghary

Abstract 2,2′-[(8-hydroxyquinolin-7-yl)methylazanediyl] diacetic acid (HQMADA) was synthesized via reaction of 8-hydroxyquinoline with iminodiacetic acid in presence of paraformaldehyde with a yield of 27%. The obtained compound was well characterized via different analytical techniques. Labeling of the synthesized compound with technetium-99m in pertechnetate form (^{99m}TcO$_4^-$) in the presence of stannous chloride dihydrate was carried out via chelation reaction. The reaction parameters that affect the labeling yield such as HQMADA concentration, stannous chloride dihydrate concentration, pH of the reaction mixture, and reaction time were studied to optimize the labeling conditions. Maximum radiochemical yield of ^{99m}Tc-HQMADA complex (91.9%) was obtained by using 1.5 mg HQMADA, 50 µg SnCl$_2$·2H$_2$O, pH 8 and 30 min reaction time. Biodistribution studies in mice were carried out in experimentally induced infection in the left thigh using *E. coli*. ^{99m}Tc-HQMADA complex showed higher uptake ($T/NT = 5.5 \pm 0.3$) in the infectious lesion than the commercially available ^{99m}Tc-ciprofloxacin ($T/NT = 3.8 \pm 0.8$). Biodistribution studies for ^{99m}Tc-HQMADA complex in Albino mice bearing septic and aseptic inflammation models showed that ^{99m}Tc-HQMADA complex able to differentiate between septic and aseptic inflammation.

Keywords Synthesis · Quinoline · Technetium-99m · Infection · Inflammation · Diagnosis

M. A. Motaleb (✉)
Labeled Compound Department, Hot Labs Center, Atomic Energy Authority, P.O. Box 13759, Cairo, Egypt
e-mail: mamotaleb@maktoob.com

E. S. Alabdullah · W. A. Zaghary
Pharmaceutical Chemistry Department, Faculty of Pharmacy, King Saud University, Riyadh, Saudi Arabia

Introduction

Infectious diseases remain a major health problem and cause of death worldwide, particularly in developing countries. Timely and specific diagnosis of infection diseases can be clinically challenging but essential for the patient's outcome. Clinicians use a variety of clues, e.g. clinical, laboratory, and radiological tests, to give a good diagnosis of infection as earlier as possible. Several imaging methods like ultrasonography (US), computer tomography (CT), and magnetic resonance imaging (MRI) are available and have been used for the past several decades for the localization of infection. But it is well known that these are not the best of methods for the localization of infection at early stages. These procedures detect the morphologic alterations of the tissues after significant process has taken place in the infective process leading to abscess formation [1]. The radiopharmaceuticals routinely used for scintigraphic detection include ^{67}Ga-citrate [2, 3] and ^{99m}Tc or ^{111}In-labelled leukocytes. ^{67}Ga-citrate has been used for identify infection for more than three decades but it presents a low specificity and exposes the patient to a high dose of radiation [4, 5]. Leukocytes labeled with ^{99m}Tc is considered "gold standard" for imaging of infections and inflammation but in vitro labeling process is labor and involves direct handling of blood potentially contaminated [4, 6].

Considering these radiopharmaceuticals disadvantages efforts has been devoted to the search of new agents for scintigraphic imaging which allows for the quick and efficient identification of inflammatory and infecious foci, with a high level of sensitivity and specificity [7, 8].

One of the most important radiopharmaceuticals that are now currently available for imaging infection is the antimicrobial agent ciprofloxacin labeled with ^{99m}Tc, which has

probably shown the best results. However, previously reported data about the labeling yield, stability and specificity of ^{99m}Tc-ciprofloxacin for infection are contradictory [1, 9–14]. Therefore, other antimicrobial agents such as levofloxacin [15], pefloxacin [16], lomefloxacin [17], cefoperazone [18], cefuroxime [19], sparafloxacin [20], difloxacin [21], and moxifloxacin [22] were labeled with ^{99m}Tc to be used for imaging sites of infection and to overcome the drawback of ^{99m}Tc-ciprofloxacin. 2, 2′-((8-hydroxyquinolin-7-yl)methyl azanediyl) diacetic acid (HQMADA) carries the pharmacophoric group iminodiacetic acid IDA (essential for complexing with ^{99m}Tc for imaging effect) is a simple broad spectrum antibacterial drug. In the present study HQMADA was synthesized, characterized and the labeling conditions for ^{99m}Tc-HQMADA complex was studied in detail and the biological distribution in inflammation bearing animals was studied.

Experimental

Melting point was determined using a Mettler FP 80 melting point apparatus and is uncorrected. The infrared spectrum (IR) was recorded on Perkin Elmer, FT-IR, using potassium bromide disc. ^{1}HNMR spectrum was recorded on a Varian XL 500 MHz FT spectrometry; chemical shifts are expressed in δ ppm with reference to TMS. Mass spectrum (MS) was performed on a Joel JMSAX 500 mass spectrometer using the electron ionization technique. Thin layer chromatography was performed on precoated (0.75 mm) silica gel GF$_{254}$ plates (E. Merck, Germany). HQMADA was detected with 254 nm UV lamp.

2,2′-[(8-Hydroxyquinolin-7-yl)methylazanediyl]diacetic acid (HQMADA)

A mixture of paraformaldehyde (0.18 g, 0.002 mol) and iminodiacetic acid (0.528 g, 0.004 mol) in DMF (25 mL) was refluxed for 30 min. 8-hydroxyquinoline (0.29 g, 0.002 mol) was added and the reaction mixture was refluxed for 24 h. The reaction mixture was concentrated under reduced pressure and then poured onto ice-water. The solid formed was filtered, washed several times with diethyl ether and crystallized from DMF (mp 210-212, yield 27%) (Fig. 1). The formed pale yellow crystal was

characterized as follow: The IR spectrum (v, cm^{-1}) exhibited bands at 2400–3667 (OH of carboxylic acid moiety and OH of quinoline ring); 1550–1621 (the carboxylate ion). Its ^{1}HNMR: δ ppm (DMSO-d$_6$) showed peaks at δ 2.7 and 2.8 (s, 4H, 2 CH$_2$–COOH), 3.4 (s, 2H, CH$_2$–N), 7.6–9 (m, 5H, aromatic protons) and 9.9 (s, 1H, aromatic C–OH). ^{13}CNMR: δ ppm (Acetic Acid) showed peaks at δ 30.69, 35.88 & 43.79 (3 × CH$_2$), 122–160.87 (aromatic carbons), 178.52 (2 × CO). Its MS showed the molecular ion peak at m/z 290.

Elemental analysis calculated for C$_{14}$H$_{14}$N$_2$O$_5$: C 57.93%; H 4.86%; N 9.65. Found: C 57.31; H 4.52; N 9. 19.

Labeling of quinoline by technetium-99m

A specific amount of HQMADA (1.5 mg) dissolved in 0.5 mL DMF and 0.5 mL phosphate buffer of pH 8 was added, 50 μL of freshly prepared deoxygenated aqueous solution of stannous chloride dihydrate and sodium pertechnetate (1–1.5 GBq) were introduced and mixed in sterile and under positive nitrogen gas pressure glass vial, closed with a rubber stopper and an aluminum cap. The mixture was agitated in a vortex mixer and left to react at room temperature (25 °C) for 30 min. The factors that affect the labeling yield like quinoline amount (0.5–2 mg), stannous chloride amount (10–100 μL), reaction time (5–120 min) and pH of the reaction mixture (2–11) were studied to optimize the reaction conditions.

### Quality control

Radiochemical yield and purity

The radiochemical yield and purity of ^{99m}Tc-HQMADA complex were determined by thin layer chromatography (TLC) and high performance liquid chromatography (HPLC).

TLC analysis

The radiochemical yield of ^{99m}Tc-HQMADA complex was determined according to the following method:

The percentage of reduced hydrolyzed technetium-99m (RH^{99m}Tc) and stannous hydroxide colloids were determined by filtration of the reaction mixture through 0.22 μm

Fig. 1 Scheme of synthesis of HQMADA
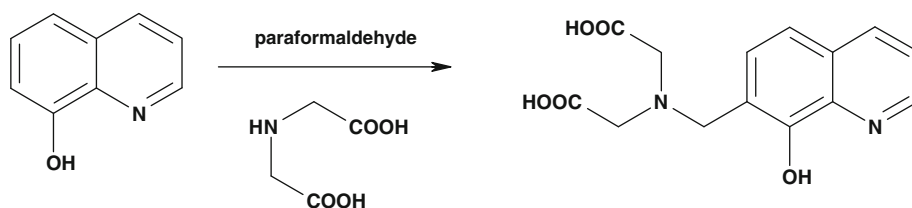
Millipore filter by using a suitable pressure. TLC-SG sheets were marked 2 cm from the base and lined into fragments 1 cm each up to 14 cm using non-pointed pencil. A spot (5 mL) from the reaction mixture obtained after filtration was applied using micropipette and then the sheet was developed in an ascending manner in a closed jar containing the developing solvent of methyl ethyl ketone (MEK). The sheets after complete development were removed, dried, and cut into strips, each strip is 1 cm width, and then the strips were counted in a well type γ-counter.

HPLC analysis

It was further confirmed by a Shimadzu HPLC system, which consists of pumps LC-9A, Rheodyne injector and UV spectrophotometer detector (SPD-6A) operated at a wavelength of 254 nm. Chromatographic analysis was performed by injection of 5 μL from the reaction mixture of HQMADA into a reversed-phase column (RP-18-250 × 4 mm, 5 μm, Lichrosorb). The column was eluted with 10% ethanol in 0.2 M phosphate buffer pH 7.2 and the flow rate was adjusted to 0.5 mL/min. Then fractions of 0.5 mL were collected separately using a fraction collector up to 14 mL and counted in a well-type γ-scintillation counter.

Stability of ^{99m}Tc-HQMADA in serum

Stability of ^{99m}Tc-HQMADA was studied in vitro by mixing 1.8 mL of normal serum and 0.2 mL of ^{99m}Tc-HQMADA complex and incubated at 37 °C for 24 h. Exactly 0.2 mL aliquots were withdrawn during the incubation at different time intervals up to 24 h and subjected to ITLC for determination the percent of ^{99m}Tc-HQMADA complex, reduced hydrolyzed technetium and free pertechnetate.

In vitro binding of ^{99m}Tc-quinoline to bacteria

Binding of ^{99m}Tc-HQMADA to both living and heat killed E. coli bacteria was assessed by the method described elsewhere [23]. Briefly, 0.1 mL of sodium phosphate buffer containing about 5 MBq of ^{99m}Tc-HQMADA complex was transferred to a test tube. Exactly, 0.8 mL of 50% (v/v) of 0.01 mol/L acetic acid in phosphate buffer containing approximately 1×10^8 bacteria was added. The mixture was incubated for 1 h at 4 °C and then centrifuged for 5 min at 2000 rpm at 4 °C. In competition experiments, bacteria were pre-incubated for 1 h with 50–100 fold excess of unlabeled HQMADA before addition of radio-labeled HQMADA. The supernatant was removed and the bacterial pellet was gently resuspended in 1 mL of ice cooled phosphate buffer and recentrifuged. The supernatant was removed and the radioactivity in the bacterial pellet was determined by a γ-counter. The radioactivity related to

bacteria was expressed in percent of the added ^{99m}Tc activity bound to bacteria with regard to total ^{99m}Tc activity.

Induction of infectious foci

A single clinical isolation of *Escherichia coli* (*E. coli*) from biological samples were used to produce focal infection. Individual colonies were diluted in order to obtain turbid suspension. Groups of three mice were intramuscularly injected with 200 μL of the suspension in the left lateral thigh muscle. Twenty-four hours required to get gross swelling in the infected thigh.

Induction of non-infected inflammation

Sterile inflammation was induced by injecting 200 μL of turpentine oil, sterilized by autoclaving at 121 °C for 20 min., intramuscularly in the left lateral thigh muscle of the mice. Two days later, swelling appeared.

Induction of heat killed E. coli (non-infected inflammation)

Sterile inflammation was induced by injecting 200 μL of heat killed *E. coli*, sterilized by autoclaving at 121 °C for 20 min., intramuscularly in the left lateral thigh muscle of the mice. Two days later, swelling appeared.

Differences in the data were evaluated with the Student t test. Results for P using the 2-tailed test are reported and all results are given as mean ± SEM. The level of significance was set at $P < 0.05$.

Results and discussion

Radiochemical purity and stability of ^{99m}Tc-HQMADA complex were assessed by thin layer chromatographic method and reversed-phase high-performance liquid chromatography. In thin layer chromatography using MEK as the developing solvent, free ^{99m}TcO$_4^-$ moved with the solvent front ($R_f = 1$), while ^{99m}Tc-HQMADA remained at the point of spotting ($R_f = 0$). Reduced hydrolyzed technetium was determined by filtration of the reaction mixture through 0.22 μm Millipore filter and the percentage of colloid was determined according to the following equation:

$$\% \text{Colloids} = \frac{\text{Activity before filtration} - \text{Activity after filtration}}{\text{Total activity}} \times 100$$

The radiochemical purity was determined by subtracting the sum of the percent of colloid and free pertechnetate
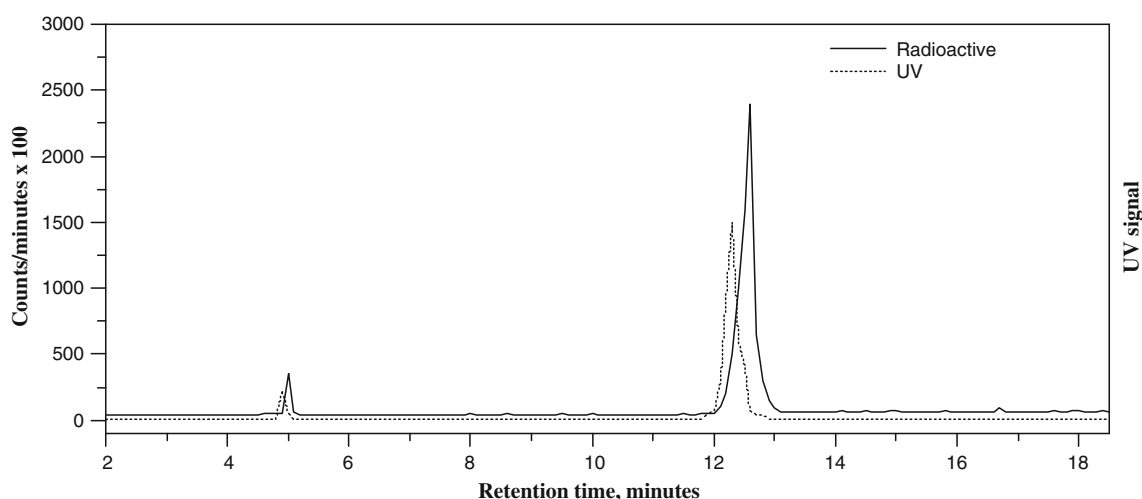
Fig. 2 HPLC radiochromatogram of ^{99m}Tc-HQMADA

from 100%. The radiochemical yield is the mean value of three experiments.

An HPLC radiochromatogram is presented in Fig. 2 and showed two peaks, one at fraction No. 5, which corresponds to ^{99m}TcO$_4^-$, while the second peak was collected at fraction No. 12.6, which corresponds to ^{99m}Tc-HQMADA complex, which was found to coincide with the UV signal.

Factors affecting the labeling yield

Effect of reaction time

The radiochemical yield of ^{99m}Tc-HQMADA was studied at different reaction times (5–60 min) in the presence of stannous chloride dihydrate and pH 8 as shown in Table 1. It is clear that the labeling yield increased from 47.5 to 91.9% by increasing the reaction time from 5 to 30 min. The radiochemical yield reaches the saturation value and is not affected by increasing the reaction time above 30 min.

Effect of HQMADA amount

The radiochemical yield of ^{99m}Tc-HQMADA, as a function of HQMADA concentration was studied as shown in

Table 1 Effect of the reaction time on the radiochemical yield of ^{99m}Tc-HQMADA

Reaction time (min)	^{99m}Tc-HQMADA (%)	^{99m}TcO$_4^-$ (%)
5	47.5 ± 1.5	52.5 ± 1.9
15	88.1 ± 2.8	11.9 ± 1.1
30	91.9 ± 3.5	8.2 ± 0.8
45	91.8 ± 3.4	8.1 ± 0.9
60	91.9 ± 3.1	8.1 ± 1

Fig. 3. The results clarify that the radiochemical yield of ^{99m}Tc-HQMADA increased from 84 to 91.9% by increasing the amounts of HQMADA from 0.5 to 1.5 mg. The amount of HQMADA higher than 1.5 mg has no effect on the labeling yield. This may be attributed to the fact that the amount of HQMADA at 0.5 mg is insufficient to shift completely the complex formation equilibrium towards the final complex, while 1.5 mg can shift it with higher efficiency. Increase in the amount of HQMADA above 1.5 mg does not modify substantially the yields.

Effect of stannous chloride dihydrate amount

For contributing most of technetium-99m to increase the labeling yield of radiopharmaceuticals, SnCl$_2$·2H$_2$O remained the best reducing agent for reduction of ^{99m}Tc from (VII) to lower valence state, which facilitates its chelation by compounds of diagnostic importance. The influence of stannous chloride amount on the labeling process was studied as shown in Fig. 4. The experiment was carried out by adding different volumes of nitrogen purged stannous chloride dihydrate solution to the solution of HQMADA and pertechnetate in closed penicillin vial (10 mL) kept under positive nitrogen gas pressure. The results clarify that the labeling yield increased from 60 to 91.9% by increasing the amount of SnCl$_2$·2H$_2$O from 10 to 50 μg. By increasing the stannous chloride amount more than 50 μg, the labeling yield decreased. This may be due to the fact that most of the ligand molecules were consumed in the formation of complexes, so the pertechnetate is reduced to insoluble technetium (IV) TcO$_2$·xH$_2$O in the absence of ligand [24] or due to the fact that the excess amount of stannous chloride leads to the formation of stannous hydroxide colloid Sn(OH)$_3^-$ in basic medium [25] as the very high Sn(II) concentration increases the reduction reaction rate to colloid formation so

Fig. 3 Variation of the radiochemical yield of ^{99m}Tc-HQMADA as a function of HQMADA concentration
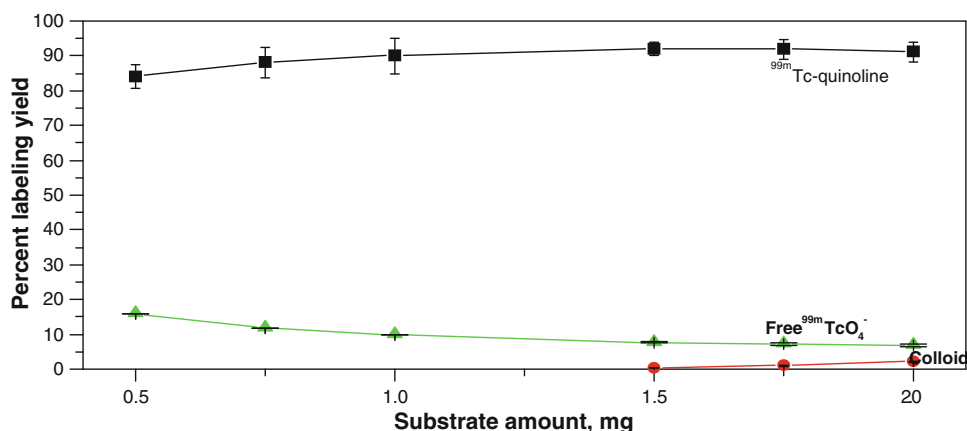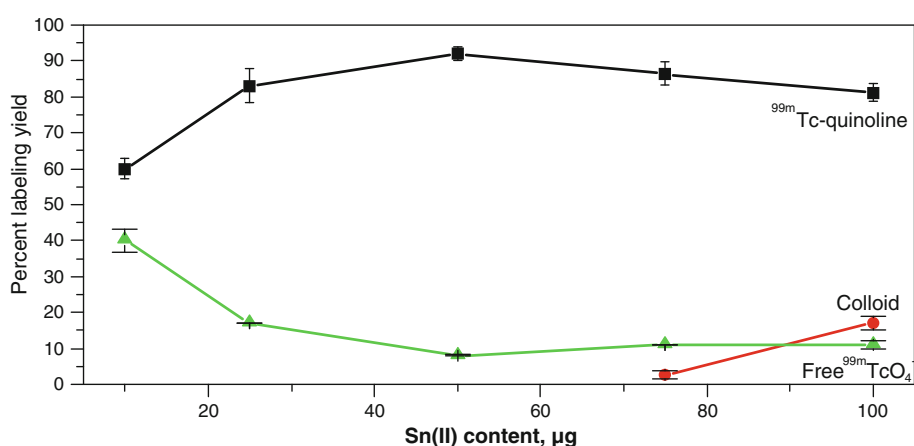

Fig. 4 Variation of the radiochemical yield of ^{99m}Tc-HQMADA as a function of stannous concentration

that it becomes more competitive with respect to the complexation reaction thus decreasing the labeling yields. Most of the radiochemical impurities found are colloids equal to 16.9% at 100 μg SnCl$_2$·2H$_2$O.

Effect of pH of the reaction mixture

The data presented in Table 2 reflect the results obtained from the labeling of HQMADA with technetium-99m at different pH values. The results confirm the influence of pH of the reaction mixture on the radiochemical yield of ^{99m}Tc-HQMADA. The percentage of ^{99m}Tc-HQMADA increased gradually with increasing the pH up to 8 to give a labeling yield of 91.9% at 25 °C within 30 min. By increasing the pH of the reaction medium above pH 8 the yield of ^{99m}Tc-HQMADA slightly decreased and reached 81% at pH 11. At low pH (pH 4), the low values of the labeling yield may be attributed to the formation of unstable ^{99m}Tc-HQMADA complexes, which decompose after destroying the reductive medium. At pH 8, the labeling yield increased to 91.9%, which may be attributed to the deprotonation of the HQMADA that is surely present

Table 2 Effect of pH of the reaction medium on the radiochemical yield of ^{99m}Tc-HQMADA

pH value	^{99m}Tc-quinoline (%)	^{99m}TcO$_4^-$ (%)
4	45.5 ± 1.5	54.5 ± 1.9
6	68 ± 2.8	32 ± 2.1
8	91.9 ± 3.5	8.1 ± 1.1
9	85.7 ± 1.9	14.3 ± 0.9
11	81 ± 2.1	19 ± 2.0

at high pH values and increased the stability of TcO(V)-(HQMADA)2 complex. Higher OH$^-$ concentration could be responsible for the partial hydrolysis of the complex and oxidation of Tc(V) to pertechnetate.

In vitro stability of ^{99m}Tc-HQMADA

The stability of ^{99m}Tc-quinoline was studied in order to determine the suitable time for injection to avoid the formation of the undesired products that result from the radiolysis of the labeled compound. These undesired radioactive products may be accumulated in non-target

organs. Table 3 clarifies the stability of ^{99m}Tc-HQMADA complex. The results show that ^{99m}Tc-HQMADA complex is stable up to 8 h.

Table 3 Stability of ^{99m}Tc-HQMADA

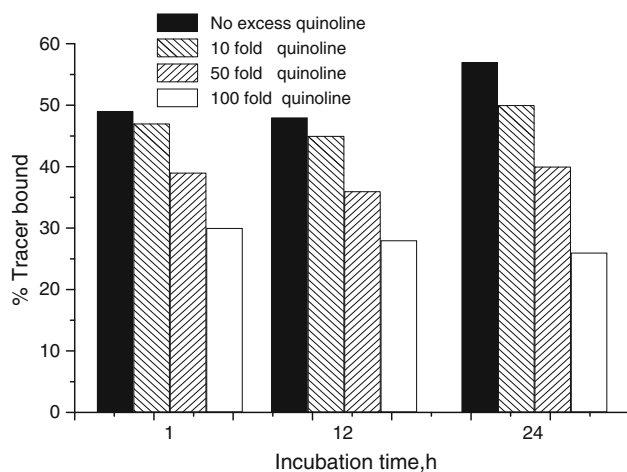| Time (h)	^{99m}Tc-quinoline (%)
1	91.8 ± 1.5
2	91.9 ± 2.8
4	91.1 ± 3.5
6	91 ± 1.9
8	89.7 ± 2.1

Fig. 5 In vitro binding of the ^{99m}Tc-HQMADA to *E. coli* (n = 4)

Stability test

Incubation of the preparation containing ^{99m}Tc-HQMADA in normal serum for 24 h at 37 °C resulted in a small release of radioactivity (8.5 ± 2.7%, $n = 5$ experiments) from the ^{99m}Tc-HQMADA, as determined by HPLC and ITLC.

In vitro binding studies

In vitro binding of ^{99m}Tc-HQMADA to bacteria (49–57%) was similar to that of ^{99m}Tc-ciprofloxacin [22] (40–65%). Competition binding of the ^{99m}Tc-HQMADA to *E. coli* was assessed by pre-incubating the bacteria with 10–100 fold excess of the unlabeled corresponding HQMADA and then assessing the amount of radioactivity bound to the bacteria. The results reveal that pre-incubating with 100-fold excess of HQMADA significantly decreased the binding of ^{99m}Tc-HQMADA to *E. coli* but in case of killed *E. coli* the added unlabelled HQMADA does not affect the binding percentage indicating that; ^{99m}Tc-HQMADA complex is a specific agent for bacterial cells Fig. 5.

Biodistribution

Data in Table 4 revealed that, after 24 h of tracer administration the major part of activity of ^{99m}Tc-HQMADA was found in liver (9.7 ± 0.4% ID) and intestine (33.7 ± 2.8% ID). The amount of accumulated activity in the left thigh inflamed tissue was nearly five and half fold higher than that in the right thigh control tissue in the live *E. coli* mice

Table 4 Biodistribution of ^{99m}Tc-HQMADA in *E. coli*, heat killed *E. coli* and turpentine oil inflamed rats at different time intervals

| Organs and body fluids	% Injected dose/organs at different time intervals (h)								
	E. coli			Heat killed *E. coli*			Turpentine oil		
	2	4	24	2	4	24	2	4	24
Inflamed muscle	1.38 ± 0.2	1.25 ± 0.11	1.15 ± 0.06	0.53 ± 0.01	0.46 ± 0.02	0.36 ± 0.0	0.63 ± 0.0	0.46 ± 0.01	0.34 ± 0.0
Control muscle	0.2 ± 50.1	0.23 ± 0.02	0.22 ± 0.0	0.24 ± 0.0	0.22 ± 001	0.2 ± 0.0	0.25 ± 0.0	0.22 ± 0.0	0.2 ± 0.0
Liver	14.9 ± 3.2	17.1 ± 2.0	9.7 ± 0.4	15.2 ± 2.4	18.3 ± 2.2	9.9 ± 0.5	15.0 ± 3.0	19.2 ± 2.2	10.2 ± 0.6
Urine	19.5 ± 3.5	27.9 ± 4.2	31.9 ± 3.1	18.1 ± 1.3	25.3 ± 1.1	32.4 ± 2.7	19.0 ± 0.9	27.4 ± 1.8	31.8 ± 2.4
Kidneys	13.2 ± 1.2	11.7 ± 1.3	7.9 ± 0.4	13.9 ± 1.3	11.2 ± 2.3	7.5 ± 0.7	14.3 ± 2.5	13.0 ± 1.2	6.9 ± 0.3
Blood	6.3 ± 0.4	4.1 ± 0.2	1.00 ± 0.0	7.10 ± 0.2	5.0 ± 0.2	1.3 ± 0.1	6.5 ± 0.2	4.3 ± 0.2	1.0 ± 0.0
Heart	0.4 ± 0.1	0.1 ± 0.0	0.09 ± 0.0	0.3 ± 0.09	0.1 ± 0.0	0.1 ± 0.0	0.4 ± 0.08	0.2 ± 0.0	0.1 ± 0.0
Lung	1.3 ± 0.2	0.3 ± 0.0	0.1 ± 0.0	1.1 ± 0.09	0.2 ± 0.0	0.1 ± 0.0	1.4 ± 0.09	0.4 ± 0.1	0.2 ± 0.0
Intestine	22.9 ± 2.5	26.1 ± 0.5	33.7 ± 0.3	22.1 ± 3.4	24.5 ± 0.4	31.2 ± 0.7	18.9 ± 1.9	21.9 ± 0.8	31.9 ± 0.4
Stomach	1.9 ± 0.02	2.3 ± 0.0	2.9 ± 0.0	1.1 ± 0.09	1.2 ± 0.0	3.1 ± 0.2	1.4 ± 0.09	2.4 ± 0.1	3.2 ± 0.0
Spleen	2.40 ± 0.1	1.20 ± 0.2	0.3 ± 0.1	2.3 ± 0.3	1.3 ± 0.0	0.5 ± 0.1	2.1 ± 0.1	1.3 ± 0.0	0.3 ± 0.0
Bone	0.90 ± 0.1	0.50 ± 0.1	0.20 ± 0.0	1.1 ± 0.0	0.5 ± 0.1	0.3 ± 0.0	1.1 ± 0.2	0.5 ± 0.1	0.1 ± 0.0
T/NT	5.52 ± 0.2	5.43 ± 0.0	5.22 ± 0.0	2.2 ± 0.09	2.1 ± 0.0	1.8 ± 0.0	2.5 ± 0.09	2.1 ± 0.1	1.7 ± 0.0
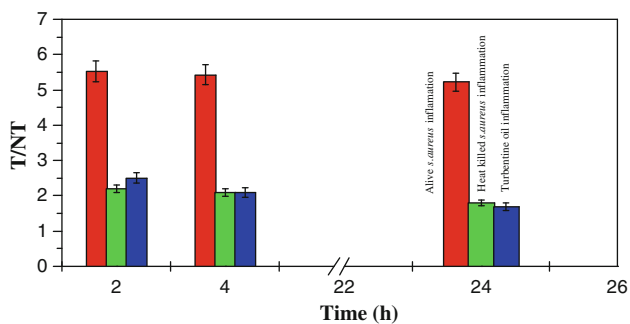
Fig. 6 The ratio of target muscle (*T*) to non target muscle (*NT*) of ^{99m}Tc-HQMADA in different inflammation models at different post injection times

model but in the turpentine oil mice model and in the killed *E. coli* mice model, the *T/NT* value was nearly equal to 2 Fig. 6. As a result ^{99m}Tc-HQMADA complex is specific agent and can differentiate bacterial infection from sterile inflammation.

Conclusion

^{99m}Tc-HQMADA complex can be prepared easily with a high labeling yield (91.9%) and stability (up to 8 h) than the commercially available ^{99m}Tc-ciprofloxacin. These findings, combined with the advantages of the high *T/NT* value and in vitro binding of ^{99m}Tc-HQMADA complex, was promising enough to state that ^{99m}Tc-HQMADA could be used instead of the commercially available ^{99m}Tc-ciprofloxacin as infection imaging agent.

References

1. Britton KE, Vinjamuri S, Hall AV (1997) Eur J Nucl Med 24:553–555
2. Seabold JE, Palestro CJ, Brown ML (1997) J Nucl Med 38:994–997
3. Staab EV, Mccartney H (1978) Semin Nucl Med 8:219–223
4. Love C, Palestro C (2004) J Nucl Med Technol 32:47–57
5. Chianelli M, Mather SJ, Martin-Comin J, Signore A (1997) J Nucl Med Commun 18:437–455
6. Corstens FHM, Van Der Meer JWM (1999) Lancet 354:765–770
7. Van Eerd JEM, Broekema M, Harris TD, Edwards DS, Oyen WJG, Corstens FHM, Boerman OC (2005) J Nucl Med 46:1546–1551
8. Laverman P, Dams ET, Oyen WJ, Storm G, Koenders EB, Prevost R, Van der Meer JW, Costens FHM, Boerman OC (1999) J Nucl Med 40:192–197
9. Pirmettis I, Limouris GS, Papadopoulos M (1999) Eur J Nucl Med 26:1108
10. Vinjamuri S, Hall AV, Solanki KK (1996) Lancet 347:233–235
11. Rien HS, Huub JR, Otto CB, Rudid D, Guido S (2004) J Nucl Med 45:2088–2094
12. Seung JO, Jin SR, Joong WS, Eun JY, Hyun JH (2002) Appl Radiat Isot 57:193–195
13. Welling MM, Lupetti A, Balter HS, Lanzzeri S, Souto B, Rey AM, Savio EO, Paulusma-Annema A, Pauwels EK, Nibbering PH (2001) J Nucl Med 42:788–790
14. Valtonen V, Karppinen L, Kariniemi AL (1989) J Infect Dis Suppl 60:79–83
15. El-Ghany EA, Amine AM, El-Kawy OA, Amin M (2007) J Labelled Comp Radiopharm 50:25–29
16. El-Ghany EA, El-Kolaly MT, Amine AM, El-Sayed AS, Abdel-Gelil F (2005) J Radioanal Nucl Chem 266:131–135
17. Motaleb MA (2007) J Radioanal Nucl Chem 272:95–98
18. Motaleb MA (2007) J Radioanal Nucl Chem 272:167–171
19. Yurt Lambrecht F, Durkan K, Unak P (2008) J Radioanal Nucl Chem 275:161–166
20. Motaleb MA (2009) J Labelled Comp Radiopharm 52:415–418
21. Motaleb MA (2010) J Labelled Comp Radiopharm 53:104–109
22. Sankha C, Sujata SD, Susmita C, Kakali D, Mridula M, Bharat RS, Samarendu S, Shantanu G (2010) Appl Radiat Isot 68:314–316
23. Welling MM, Paulusma-Annema A, Balter HS, Pauwels EKJ, Nibbering PH (2000) Eur J Nucl Med 27:292–296
24. Srivastava SC, Richards P (1983) Technetium-labled compounds. In: Rayudu GVS (ed) Radiotracers for medical applications, CRC series in radiotracers in biology and medicine. CRC Press, Boca Raton, pp 107–185
25. Wardell JL (1994) Tin: inorganic chemistry. In: King RB (ed) Encyclopedia of inorganic chemistry, vol 8. Wiley, New York, pp 4159–4197